ResearchGate

See discussions, stats, and author profiles for this publication at: https://www.researchgate.net/publication/338833326

Experimental Analysis of Impact of Seepage Velocity on Mass Flux of Seawater in Coastal Aquifers

Research · November 2019

CITATIONS
0

READS
152

4 authors:



Oludotun OMONIYI Faluyi
Kwara State University
5 PUBLICATIONS **1** CITATION
SEE PROFILE



Olufemi S. Bamigboye
Kwara State University
20 PUBLICATIONS **69** CITATIONS
SEE PROFILE



Toba EMMANUEL Bamidele
Kwara State University
11 PUBLICATIONS **42** CITATIONS
SEE PROFILE



Taofeeq Ayinde Issa
Kwara State University
11 PUBLICATIONS **3** CITATIONS
SEE PROFILE

All content following this page was uploaded by Olufemi S. Bamigboye on 27 January 2020.

The user has requested enhancement of the downloaded file.

Journal of Hydrogeology & Hydrologic Engineering

Research Article

A SciTechnol Journal

Experimental Analysis of Impact of Seepage Velocity on Mass Flux of Seawater in Coastal Aquifers

Oludotun Omoniyi Faluyi[1]*, Olufemi Sijuade Bamigboye[2], Toba Emmanuel Bamidele[2] and Taofeeq Ayinde Issa[2]

Abstract

Excessive abstraction of freshwater at coastal regions may reverse the direction of flow of mass flux of dissolved salts (*J*) leading to Saltwater Intrusion (SI) contaminating freshwater in coastal aquifers. This work investigated the impact of seepage velocities and hydraulic gradients of various porous media on mass flux of saltwater contaminant. Darcy's and Fick's laws were used to develop a model which gives *J* as a function of seepage velocity (*V*) and hydraulic gradient *i*. In validating the model, an experiment was designed to determine *J* in which river bed sand were washed, dried and sieved into five different grain sizes of samples A(least Ø),B,C,D and E(greatest Ø) using electric sieve with mesh ranged150-500 µm. The Ø of each sample was determined using volumetric technique. Two vertical arms of calibrated cylinder glass with diameter 1.2 × 10^{-2}m were joined with a similar glass cylinder in the horizontal position which housed the samples. Samples screened at both ends of length *x* were inserted into the glass with air completely eliminated using displacement method before commencement of flow experiment. The *V* and *i* were determined for five samples after which *J* was determined at interface and at other points. The values of seepage velocity V, mass flux J and hydraulic gradient I for various samples at time intervals of 60 seconds to 300 seconds were obtained from the experimental procedure. The plots of Seepage Velocity V against Mass flux showed increase in seepage velocity with mass flux but there is a limit point at which the seepage velocity decreases with increase in mass flux. The results confirmed that the hydraulic gradient required to drive the mass flux through the samples reduce with increase in porosity.

Keywords

Abstraction; Aquifers; Seepage velocity; Mass flux; Hydraulic gradient

Introduction

Population growth and agricultural development in coastal areas have increased the demand for freshwater. As a result of this demand more stress is being placed on coastal aquifers. Saltwater intrusion is the most common contamination problem in coastal aquifers and a major constraint imposed on groundwater utilization [1]. Saline contamination of freshwater resources can cause significant social, economic and environmental hazards. When pumping takes place in excess of replenishment, the drawdown of the water table creates a piezometric head, the fresh water becomes less than the adjacent salt water wedge. Then the saline water moves inland causing a saltwater intrusion. The saltwater may reach the well which becomes contaminated. Saltwater intrusions have occurred in many coastal aquifers.

The extent of saltwater intrusion into an aquifer depends on several factors, including the total rate of groundwater that is withdrawn from an aquifer compared to the total freshwater recharge to the aquifer; the distance between the locations of groundwater discharge such as pump age from wells and drainage to canals and the source (or sources) of saltwater; the geologic structure of an aquifer or aquifer system (including structural features such as faults, folds, and bounding submarine canyons); the distribution of hydraulic properties of an aquifer (including the interconnectivity of coarse-grained units within multi-layered aquifer systems) and the presence of confining units that may prevent saltwater from moving vertically toward or within the aquifer [2]. Many authors have recognized that there may be multiple sources of salinity to coastal aquifers, and that it can be difficult to unequivocally delineate the specific sources of salinity in a particular aquifer. Although there are concurrent sources of potential salinity in several of the cases discussed here the discussion is focused on saltwater intrusion that has been shown to have been caused by the movement of saline water into or within coastal aquifers in response to Anthropogenic stresses [3]. As solute in saturated porous medium is adverted by the fluid flowing through it, the fluid velocity needs to be described to study contaminant transport. The pore-scale fluid velocity is spatially varying due to three interrelated reasons:

1. The no-slip condition renders the fluid velocity zero at the solid surfaces and the larger velocities occur away from the solid surfaces
2. Complex pore-scale geometry and interconnectedness
3. Variability of pore-sizes. Because of these factors, describing in detail the fluid velocity at the pore-scale is a difficult task. However, the flux of fluid over cross-sections containing many pores-spaces has been experimentally shown to follow Darcy's law [4].

The hydraulic head represents the potential energy of the subsurface water at any given point and is determined from the water level pressure and elevation of the point relative to a specified datum [5]. Groundwater flows from a high hydraulic head to a lower hydraulic head [6]. The hydraulic gradient is simply the loss of head per unit length of flow along a stream line and it is the measure of the change in hydraulic head (*dh*) across a given distance (*dl*).

In the developed model $j = vC_o \exp\left(\frac{-v}{D_o}\right)x$, the simulated mass flux was determined by using properties of the medium such as seepage velocity *v*, effective diffusion coefficient D_o and initial concentration C_o that were obtained empirically [7]. The objective of this work is to investigate the impact of seepage velocity and hydraulic gradient on mass flux of saltwater using experimental model.

***Corresponding author:** Oludotun Omoniyi Faluyi, Department of Physics and Materials Science, Kwara State University, Malete, Kwara State, Nigeria, Tel: +234 8033772597; E-mail: oludotunfaluyi@gmail.com

Received: November 06, 2019 **Accepted:** November 21, 2019 **Published:** November 29, 2019

SciTechnol International Publisher of Science, Technology and Medicine

All articles published in Journal of Health Informatics & Management are the property of SciTechnol, and is protected by copyright laws. Copyright © 2019, SciTechnol, All Rights Reserved.

Theoretical Background

The basic equations of steady-state groundwater flow are presented below for better understanding.

Bernoulli's equation

As it is well known from fluid mechanics, for steady flow of non-viscous incompressible fluids, Bernoulli's equation

$$\frac{p}{\gamma_w}+z+\frac{v^2}{2g}=constant\ h \quad (1)$$

h=total head, ft

p=pressure, lb/ft^2

γ_w=unit weight of fluid, lb/ft^3

g=gravitational constant

v=seepage velocity, ft/sec

Demonstrates that the sum of the pressure head, p/γ_w, elevation head, z, and velocity head, at any point within the region of flow is a constant.

To account for the loss of energy due to the viscous resistance within the individual pores, Bernoulli's equation is taken as

$$\frac{P_A}{\gamma_w}+Z_A+\frac{V_A^2}{2g}=\frac{P_B}{\gamma_w}+Z_B+\frac{V_B^2}{2g}+\Delta h \quad (2)$$

Where

Δh represents the total head loss (energy loss per unit weight of fluid) of the fluid over the distance Δs. The ratio

$$i=-\lim_{\Delta s}\frac{\Delta h}{\Delta s}=-\frac{dh}{ds} \quad (3)$$

is called the hydraulic gradient and represents the space rate of energy dissipation per unit weight of fluid.

In most problems of interest the velocity heads (the kinetic energy) are so small they can be neglected. For example, a velocity of 1 ft/sec, which is large compared to typical seepage velocities through soils, produces a velocity head of only 0.015 ft. Hence, Equation (2) can be simplified to

$$\frac{P_A}{\gamma_w}+Z_A=\frac{P_B}{\gamma_w}+Z_B+\Delta h \quad (4)$$

and the total head at any point in the flow domain is simply

$$h=\frac{P}{\gamma_w}+Z \quad (5)$$

Darcy's law

The flow of groundwater is taken to be governed by Darcy's law, which states that the velocity of the flow is directly proportional to the hydraulic gradient. A similar statement in an electrical system is Ohm's law and in a thermal system, Fourier's law. The grandfather of all such relations is Newton's law of motion.

$$V=Ki=-K\frac{dh}{ds} \quad (6)$$

Equation (6), commonly called Darcy's law, demonstrates a linear dependency between the hydraulic gradient and the discharge velocity V. The discharge velocity, V is the product of the porosity n and the seepage velocity, The coefficient of proportionality K in Equation (6) is called by many names depending on its use; among these are the coefficient of permeability, hydraulic conductivity, and permeability constant. As shown in Equation (6), K has the dimensions of a velocity. It should be carefully noted in this equation that flow is a consequence of differences in total head and not of pressure gradients.

This is demonstrated in Figure 1 where the flow is directed from A to B, even though the pressure at point B is greater than that at point A.

Defining Q as the total volume of flow per unit time through a cross-sectional area A, Darcy's law takes the form

$$Q=AV=AKi=-AK\frac{dh}{ds} \quad (7)$$

Darcy's law offers the single parameter K to account for both the characteristics of the medium and the fluid.

Methods and Materials

Sample collection and preparation

Soil sample was collected in a stream at Tanke, Ilorin Kwara State close to University of Ilorin. The sample was washed and rinsed using clean water and in the process fine organic materials floated and were easily washed off. This action is necessary so as to avoid swelling and to ascertain that no any other material is present except sand. The sample was sieved into five different grain with sizes of 125, 250, 350, 400 and 450 μm and the grain sizes were tagged samples A, B, C, D and E, respectively. The porosity (Ø) of the samples A, B, C, D and E were determined using volumetric method [8].

Experimental procedure

The experimental setup consisted of two arms of calibrated cylinder glass with diameter 1.2 x10^{-2} m erected vertically and joined together with a similar glass cylinder in the horizontal position which housed the samples. Saturated sample A of length x with air completely eliminated was inserted into the horizontal glass and screened at both ends before commencement of the experiment. Freshwater was

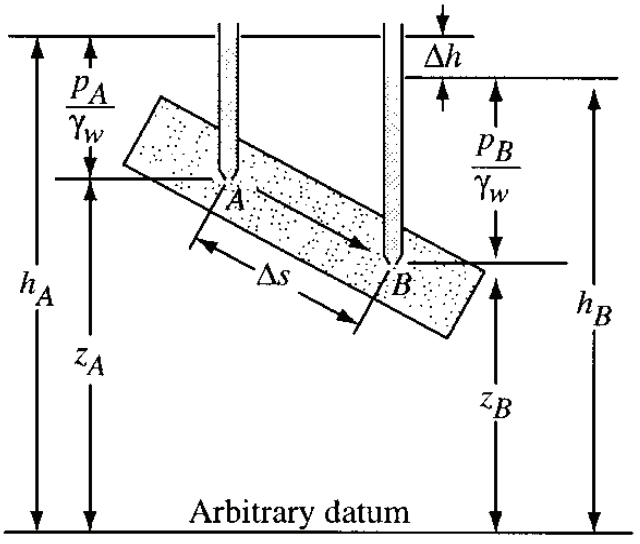


Figure 1: Heads in Bernoulli's equation.

filled in the arm labeled M to 27 cm mark and saltwater which was colored with red dye (neutral pigment) was filled in the arm labeled N to 15 cm mark. The controls were opened at the same time to allow flow to occur. The volume of freshwater displaced volume of saltwater in the setup because of the difference in the hydraulic heads of freshwater and saltwater. The flow occurs from high hydraulic head to low hydraulic head. The hydraulic gradient between freshwater and saltwater was obtained by determining the difference between hydraulic heads of freshwater and saltwater and then divided by the flow length X between the two heads. The volumetric flow rate was computed from volume of fluid displaced between the two arms per time taken and it was denoted as Q with unit of m^3s^{-1}. Darcy flux (volume flux) was obtained by dividing the volumetric flow rate with cross sectional area of the tube and it was denoted as v_x with unit of ms^{-1}, v_x=Q/A (Where A is cross sectional area of the cylindrical glass which is $\frac{\pi d^2}{4}$ and d is the diameter of the cylindrical glass, given as 1.2×10^{-2} m). The flow length X was determined from the distance of the movement of the red dye from the interface of freshwater and saltwater. The seepage velocity (V) which is the average velocity of water flow through the pores was determined by dividing the volume flux (v_x) by porosity (Ø). The mass flux of saltwater contaminant in the controlled experiment was determined using the following steps:

I. By multiplying the volumetric flow rate Q with time (t) in second to give volume of contaminated fluid displaced within the columns.

II. The mass of contaminated water displacement was obtained from the density (concentration) formula i.e mass of contaminated water displacement=density (concentration) of contaminated water × volume displacement

III. The mass flux (J) of saltwater contaminant within the columns was arrived at by dividing the mass of contaminated water displacement of saltwater with cross sectional area (A) in m^2 and time (t) taken in second i.e. unit of J is kg $m^{-2}s^{-1}$

The procedure was repeated for samples B, C, D and E. The hydraulic gradient i, volumetric flow rate Q, volume flux v_x, seepage velocity V and mass flux J for each sample were determined.

Results and Discussion

Tables 1-6 shows the porosity (Ø), hydraulic gradients (i), seepage velocity (V) and mass flux (J) between freshwater and saltwater in samples A, B, C, D and E within time interval of 60 seconds to 360 seconds respectively. It was observed that the hydraulic gradients decrease with increase in porosities and mass flux of contaminant whereas seepage velocities increase to certain limit and later decrease for all samples at time intervals of 60 seconds to 360 seconds.

The results from the experiment showed that hydraulic gradient for samples A, B, C, D and E are 3.960, 1.430, 0.635, 0.480 and 0.323 while the corresponding values of contaminant mass flux are 0.2114, 0.4420, 0.6724, 0.7592 and 0.8456 Kg $m^{-2}s^{-1}$, respectively within time interval of 60 seconds in Table 1. The results of hydraulic gradient and mass flux follow same trend for samples A, B, C, D and E at other time intervals of 120, 180, 240, 300 and 360 seconds in Tables 2-6. Hence, it showed that energy known as hydraulic gradient required in overcoming hydraulic resistance is high when porosity is low whereby ftThe conftamfinanft mass flux fis reduced vfice versa.

Table 1: Values of Porosity (Ø), Hydraulic gradient (i), Seepage velocity (V) and Mass Flux (J) at 60 seconds.

Sample	Porosity (Ø)	Hydraulic gradient (i)	Seepage Velocity (V) (ms^{-1}) × 10^{-4}	Mass Flux (J) ($Kgm^{-2}s^{-1}$) × 10^{-1}
A	0.250	3.960	8.252	2.114
B	0.300	1.430	14.325	4.420
C	0.330	0.635	19.879	6.724
D	0.375	0.480	19.752	7.592
E	0.420	0.323	19.643	8.456

Table 2: Values of Porosity (Ø), Hydraulic gradient (i), Seepage velocity (V) and Mass Flux (J) at 120 seconds.

Sample	Porosity (Ø)	Hydraulic gradient (i)	Seepage Velocity (V) (ms^{-1}) × 10^{-4}	Mass Flux (J) ($Kgm^{-2}s^{-1}$) × 10^{-1}
A	0.250	2.444	8.000	2.050
B	0.300	0.832	12.917	3.972
C	0.330	0.412	15.546	5.258
D	0.375	0.307	15.008	5.768
E	0.420	0.200	14.583	6.278

Table 3: Values of Porosity (Ø), Hydraulic gradient (i), Seepage velocity (V) and Mass Flux (J) at 180 seconds.

Sample	Porosity (Ø)	Hydraulic gradient (i)	Seepage Velocity (V) (ms^{-1}) × 10^{-4}	Mass Flux (J) ($Kgm^{-2}s^{-1}$) × 10^{-1}
A	0.250	1.651	7.875	2.018
B	0.300	0.614	11.094	3.411
C	0.330	0.296	12.784	4.324
D	0.375	0.218	12.131	4.663
E	0.420	0.137	11.607	4.997

Table 4: Values of Porosity (Ø), Hydraulic gradient (i), Seepage velocity (V) and Mass Flux (J) at 240 seconds.

Sample	Porosity (Ø)	Hydraulic gradient (i)	Seepage Velocity (V) (ms^{-1}) × 10^{-4}	Mass Flux (J) ($Kgm^{-2}s^{-1}$) × 10^{-1}
A	0.250	1.162	7.800	1.999
B	0.300	0.496	9.625	2.960
C	0.330	0.222	10.909	3.690
D	0.375	0.161	10.205	3.922
E	0.420	0.099	9.643	4.151

Table 5: Values of Porosity (Ø), Hydraulic gradient (i), Seepage velocity (V) and Mass Flux (J) at 300 seconds.

Sample	Porosity (Ø)	Hydraulic gradient (i)	Seepage Velocity (V) (ms^{-1}) × 10^{-4}	Mass Flux (J) ($Kgm^{-2}s^{-1}$) × 10^{-1}
A	0.250	0.889	7.500	1.922
B	0.300	0.428	8.438	2.595
C	0.330	0.190	9.375	3.171
D	0.375	0.132	8.755	3.365
E	0.420	0.072	8.259	3.556

Table 6: Values of Porosity (Ø), Hydraulic gradient (i), Seepage velocity (V) and Mass Flux (J) at 360 seconds.

Sample	Porosity (Ø)	Hydraulic gradient (i)	Seepage Velocity (V) (ms^{-1}) × 10^{-4}	Mass Flux (J) ($Kgm^{-2}s^{-1}$) × 10^{-1}
A	0.250	0.727	7.072	1.812
B	0.300	0.381	7.500	2.306
C	0.330	0.167	8.198	2.773
D	0.375	0.116	7.608	2.925
E	0.420	0.063	7.142	3.075

A plot was prepared between the seepage velocity V and the mass flux J. It was found to be related in polynomial of degree two

within time intervals of 60 to 360 seconds as shown in Figures 2-7. The equations obtained from the graphs can be used to predict the limit seepage velocity at which seepage velocity increase with mass flux. Table 7 shows the limit seepage velocity and the corresponding mass flux within time intervals of 60 to 360 seconds. Figure 8 shows a straight line graph of mass flux against limit seepage velocity within time intervals of 60 to 360 seconds. From Tables 1-6, seepage velocity below limit seepage velocity and corresponding mass flux can be inferred. The plots of mass flux versus seepage velocity below limit seepage velocity follow the same pattern with Figure 8. The concentration of the contaminant was obtained from the slope of

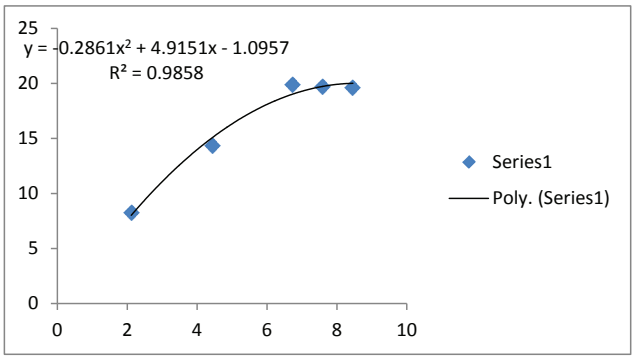


Figure 2: Plot seepage velocity V against mass flux J at 60 seconds.

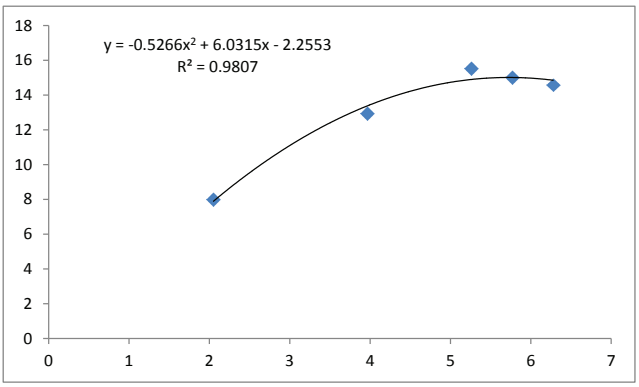


Figure 3: Plot seepage velocity V against mass flux J at 120 seconds.

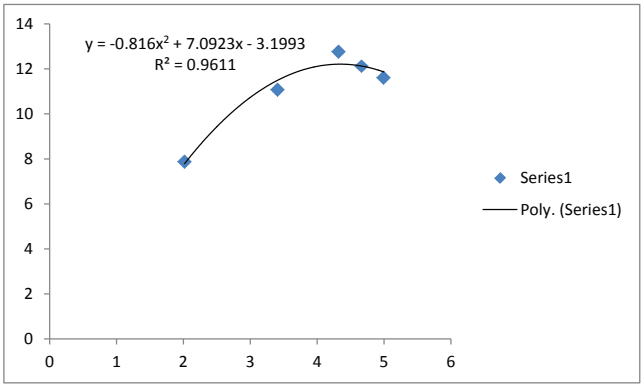


Figure 4: Plot seepage velocity V against mass flux J at 180 seconds.

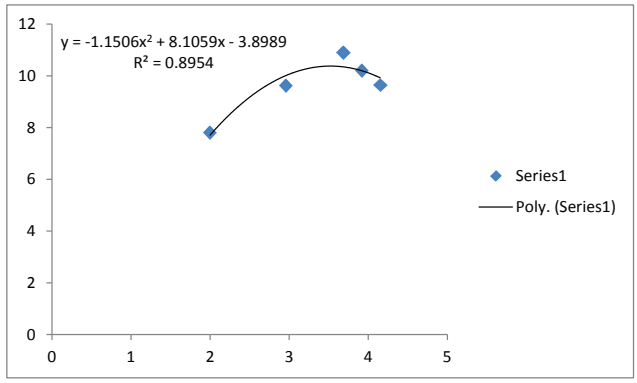


Figure 5: Plot seepage velocity V against mass flux J at 240 seconds.

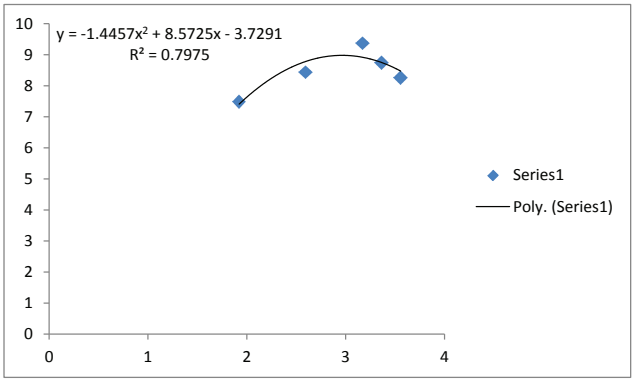


Figure 6: Plot seepage velocity V against mass flux J at 300 seconds.

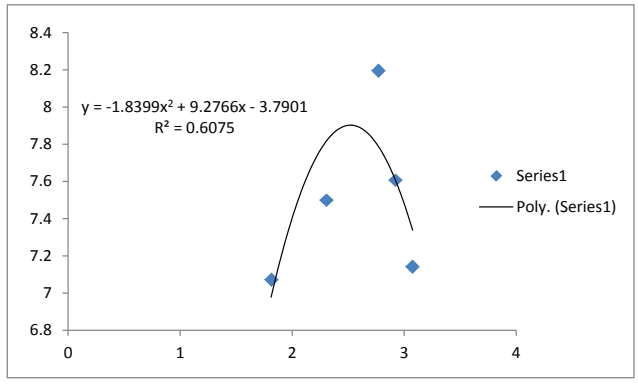


Figure 7: Plot seepage velocity V against mass flux J at 360 seconds.

Table 7: Values of Limit Seepage velocity (V) and Mass Flux (J) at 60 to 360 seconds.

Time (Second)	Limit seepage velocity (V) (ms^{-1}) × 10^{-4}	Mass flux (J) ($Kgm^{-2}s^{-1}$) × 10^{-1}
60	19.879	6.724
120	15.546	5.258
180	12.784	4.324
240	10.909	3.690
300	9.375	3.171
360	8.198	2.773

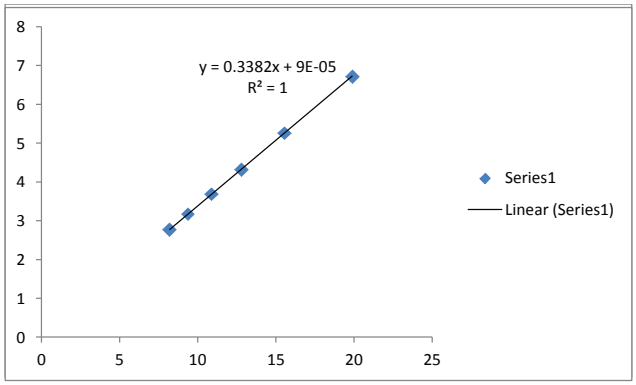


Figure 8: Plot mass flux J against limit seepage velocity V at 60 to 360 seconds.

the graph. Therefore, flow rate of saltwater contaminant between saltwater column and freshwater column depends on hydraulic gradient and seepage velocity of the samples.

Conclusion

Experimental investigation was carried out to establish the impact of seepage velocity and hydraulic gradient on the mass flux of saltwater contaminant in coastal aquifers. The results obtained indicated that seepage velocity increases with mass flux in a parabolic curve with a limit seepage velocity and beyond this limit the seepage velocity will not be proportional to the mass flux for time intervals of 60 seconds to 360 seconds. The limit seepage velocity occurred when porosity of the sample was 0.330 for all time intervals. The limit seepage velocity decreases with increase in time whereas the limit seepage velocity decreases with decrease in mass flux. Any sample with porosity less than 0.330, its seepage velocity decreases with mass flux or its seepage velocity increases with mass flux. The plot of mass flux against seepage velocity gives a straight line and the slop of the line is the concentration of the saltwater contaminant through the sample. The concentration of the contaminant is low in a sample with low porosity. The mass flux of contaminant depends on the hydraulic gradient of the fluid through which the contaminant is conveyed.

References

1. Bear J, Cheng AHD, Sorek S, Ouazar D, Herrera I (1999) Seawater intrusion in coastal aquifers - concepts, methods and practices.
2. Freeze RA and Cherry JA (1979) Groundwater. pp: 375 – 379.
3. Barlow PM (2003) Ground water in fresh water-salt water environments of the Atlantic Coast. US Geological Survey Circular.
4. Delleur JW (1999) The Handbook of Groundwater Engineering.
5. Younger PL (2007) Groundwater in the Environment: an introduction.
6. Bear J (2007) Hydraulics of groundwater.
7. Adegoke JA, Popoola OI, Faluyi OO (2019) Effect of geophysical parameters on attenuation of contaminant in freshwater coastal aquifers. J Eng Stud Res 25: 7- 15.
8. Domenico PA, Schwartz FW (2000) Physical and chemical hydrogeology.

Author Affiliations

Top

[1]*Department of Physics and Materials Science, Kwara State University, Malete, Kwara State, Nigeria*
[2]*Department of Geology and Mineral Sciences, Kwara State University, Malete, Kwara State Nigeria*

Submit your next manuscript and get advantages of SciTechnol submissions

- 80 Journals
- 21 Day rapid review process
- 3000 Editorial team
- 5 Million readers
- More than 5000 facebook fans
- Quality and quick review processing through Editorial Manager System

Submit your next manuscript at ● www.scitechnol.com/submission

View publication stats